Micro Forest Fire Detection

A Senior Project
presented to
the Faculty of the Electrical Engineering Department
California Polytechnic State University, San Luis Obispo

In Partial Fulfillment
of the Requirements for the Degree
Bachelor of Science in Electrical Engineering

by

John Cape

June, 2010

Table Of Contents

Table Of Figures

Acknowledgements

First I would like to acknowledge my colleagues, Ryan Radjabi, and Bryce Du. Without all of their work none of this system would have ever left the drawing board. Second, I would like to thank Dr. John Sahgri, for being a constant source of information and assistance as we developed these tests. Next I would like to thank Dr. John Jacobs and Raytheon. Their support and funding made this project possible. Lastly, but certainly not least, I would like to thank my parents and all my friends for supporting me throughout my entire college career and my senior project.

Introduction

From 2000 to 2008, wildfires and forest fires cost the United States an average of $733.15 million dollars per year in property and crop damage (NOAA), and an average of $900 million dollars per year in firefighting costs (Young, 2006). If a system could be designed to reduce the number of fires by early detection these costs could be greatly reduced. Our designed system is intended to use ground-based cameras to automatically detect wildfires as they start, allowing fire department resources to respond to them and contain them before they are able to burn large areas of wild land or habited areas. This system would be tested in a small trial environment in the Santa Barbra area of California's central coast before expanding to cover other major wild land areas in the United States.

Background information

For this project, we are using the spectral emissions of a forest fire to detect them. In order to properly design a system to detect fires, the process by which energy is emitted from objects must first be examined. The basis of spectral emission is Wien's law. This law states that the peak wavelength of light that an object radiates in meters is a function of the temperature in Kelvin of that object.

$$\lambda_{max}(m) = \frac{2.897 \times 10^{-3}(mK)}{T(K)}$$

This peak frequency lets us select the band of the electromagnetic spectrum that we are interested in examining. The spectrums of light that we are interested in for this project are the visible range, the short wave infrared band (SWIR), the mid infrared band (MWIR) and the thermal infrared band (LWIR). The values of the boundaries of these bands depend on the reference material used. From *Remote Sensing and Image Interpretation* the visible range is 350 to 750nm, the SWIR band is, 1.3 to 3µm, the MWIR band, from 3 to 5 µm, and LWIR band from 7.5 to 13 µm. The reason there is a gap between the

MWIR band and the LWIR band is due to atmospheric absorption. From 5 to 7µm, the water in the atmosphere absorbs the majority of transmitted radiation. This is one of the largest absorption bands in the atmosphere. There are other bands that are absorbed, such as the ozone absorption band around 9 µm, but the magnitude of the attenuation is small enough that those wavelengths are still useable for remote sensing.

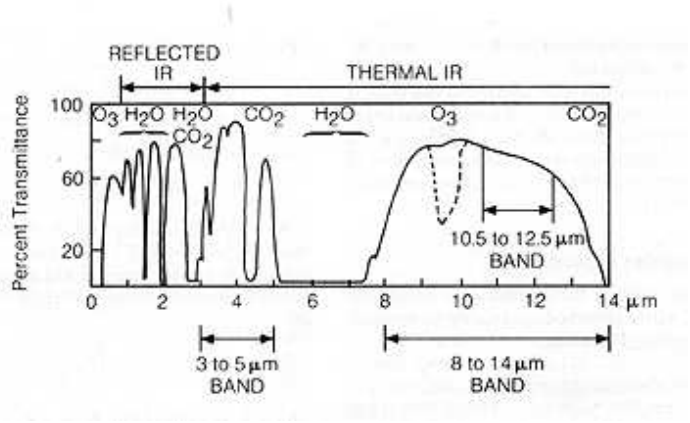

Figure 1: Atmospheric Transmission with Respect to Wavelength

Another important consideration is the minimum detectable feature size. This is based on the size of the pixel on the camera, the focal length of the lens, and the distance from the camera to the target of interest. The ratio that defines the minimum feature size is $Pixel\ Size/Focal\ Length = \frac{Minimum\ Feature\ Size}{Distance\ to\ Feature}$. This formula allows you to plug in the physical features of the system and determine the smallest object in the area of the target that will show up as one pixel in the resulting image. This is important to know, because knowing the size of the object in pixels, and the size of each pixel allows you to calculate the physical size of the object. The ability to calculate the size of an object allows you to set size detection thresholds for image processing.

Detector Types

The two types of detectors are used in this project charge coupled devices (CCD) and microbolometers. These two camera constructions achieve similar effective results, but work by different physical process. A CCD is composed of an array of capacitors, each corresponding to a single pixel. As light strikes the array, the energy from the photons separate electrons and holes. These electrons charge the capacitor. When the desired exposure time has elapsed, the voltage charges on the capacitors are shifted along their rows, read and digitized. The wavelengths that are absorbed by a particular CCD sensor depend on the bandgap of the material that the substance is made of. CCD's constructed of silicon are sensitive from approximately 300nm to 1µm. Other materials have different bandgaps. Mercury cadmium telluride (HgCdTe) is another example substrate. It is sensitive to the thermal infrared band. Because CCD's made of silicon are sensitive to the visible range of light, and silicon is already used for the majority of semiconductor devices, silicon CCDs are used in all consumer digital cameras.

The other type of detector used is a microbolometer. A microbolometer is different from a CCD in that it does not directly convert light energy to a voltage. This detector type is only used for thermal imaging. Pixels' on a microbolometer consist of an array of infrared absorbing materials. When the thermal energy hits the pixel, it is absorbed by the absorption material, and the pixel changes temperature. As the temperature of the absorber changes, the resistance changes as well. The resistance of the pixel is measured, and that resistance value is converted into an equivalent intensity. Because there are more steps required to translate the energy intensity into a visible picture, microbolometers are less sensitive and less accurate than CCD based systems.

Microbolometers are used because for the thermal band, a HgCdTe based CCD must be cooled to cryogenic temperatures of approximately 77K in order to reduce the thermal noise of the system enough to acquire useable data. The machinery required to achieve this is bulky, expensive, and difficult

to maintain. This results in CCD based infrared systems being too costly to use for most applications. In a controlled laboratory setting, they are used due to their higher accuracy. In industrial, commercial and military applications however, microbolometers are used because they are less expensive and more robust. Mid wave infrared detectors also must be actively cooled, resulting in many of the same problems.

System Specifications

There were many factors that had to be considered when creating specifications for a cost effective fire detection system. One factor was detection range. For the system to be usable in the field, each system must be able to effectively provide cover for a large enough area. Another consideration is cost. The lower the cost of each individual unit, the more units can be placed into operation, providing greater coverage to an area. The design specifications are listed in Figure 2.

Desired Detection Range	1 km
Minimum Fire Size	1 meter

Figure 2: Initial Design Requirement

Initial Design Choices

In order to decide what camera to use, we had to examine the spectral emissions a fire emits. By looking at the frequencies of maximum emission, the radiated energy is detectable at a farther range than if we examined spectral bands with lower emitted energy. Ideally, we would like to use the entire

IR band from 1µm to 15µm. is not possible because of the water absorption gap. This means that any detectors sensitive to these wavelengths would not receive any light intensity on them in the 5-7µm range, even if those frequencies are emitted by the fire. The second reason is that there is no suitable detector that can receive a band of frequencies that wide. The bandwidth of a detector is again related to the material the sensor is made of.

The first parameter we looked at is the spectral emission of a forest fire. The vast majority of fire research in literature describes satellite based systems. According to (Sun, et al., 2006) the optimal band for fire detection is 4.34-4.76 µm. Unfortunately this is in the MWIR band, where detectors are expensive and must be actively cooled. This makes them unsuitable for an application such as cost effective fire detection, where the unit must be placed out in the field with little maintenance or infrastructure for long periods of time. Therefore, a combination of other bands must be used. The possible usable bands for fire detection are ones for which uncooled detectors are available. This means that the visible light spectrum, the SWIR and the LWIR bands are potential candidates.

Knowing the available camera types, the cameras to be used can be decided. Off the shelf consumer cameras are inexpensive, but have a spectral response limited to the visible light spectrum. Thermal cameras have sensitivity in the IR range of light, but are much more expensive. In order to reliably detect a fire, we need to be able to see the fire in a wide variety of conditions. The system has to be able to see through inclement weather effects, and work at night, as well as day. The first camera system we decided to test was a standard off the shelf consumer camera. The model that was chosen was the Canon Powershot A95. Figure 3 contains the specifications for this camera.

Sensor Type	5.0 MP 1/1.8 inch type Charge Coupled Device
Effective Pixels	5.0 Million (2592x1944)
Lens Focal Length	38-114mm, f/2.8

Figure 3: Canon Powershot A95 Specifications

This camera was chosen because it was already owned, and therefore incurred no additional cost or purchasing delay to the initial testing. A filter that blocks light in the visible range was also used to attempt to increase the performance of this camera. The filter is a Harrison Duraline filter. This filter blocks wavelengths less than 670 nanometers. The filter blocks the majority of the visible range light, and lets the near infrared light that the camera is sensitive to through. This allows the camera to have a longer exposure time, and absorb more light in the IR band without saturating the sensor.

Our second camera to test was a FLIR Photon 320 camera. This camera is sensitive to the LWIR band of the electromagnetic spectrum. Its specifications are listed below in Figure 4.

Sensor Type	VOx Microbolometer
Resolution	324x256
Pixel Size	38 µm
Spectral Band	7.5-13.5µm

Figure 4: FLIR Photon 320 Specifications

We did not have access to a SWIR camera during the initial phase of our experimentation and design.

Experimental Testing

Initial Testing

Our initial testing was done on a small scale on February 12, 2010, using flame sources, as opposed to actual wood fires. This allowed us to get information on the thermal sensitivity of our cameras without having to find a location where a full scale fire could safely be set. The results of these tests showed that with both of the systems, the flame image was extremely bright compared to the surrounding environment. The thermal camera showed even more promising result than the visible camera. As seen in Figure 6, a plume of hot gas rising from the flame is clearly visible. This is the result we had hoped to see with the LWIR camera. With this short range test, we have demonstrated that a plume of gas generated by a fire, and that the IR camera can detect it, given sufficient intensity.

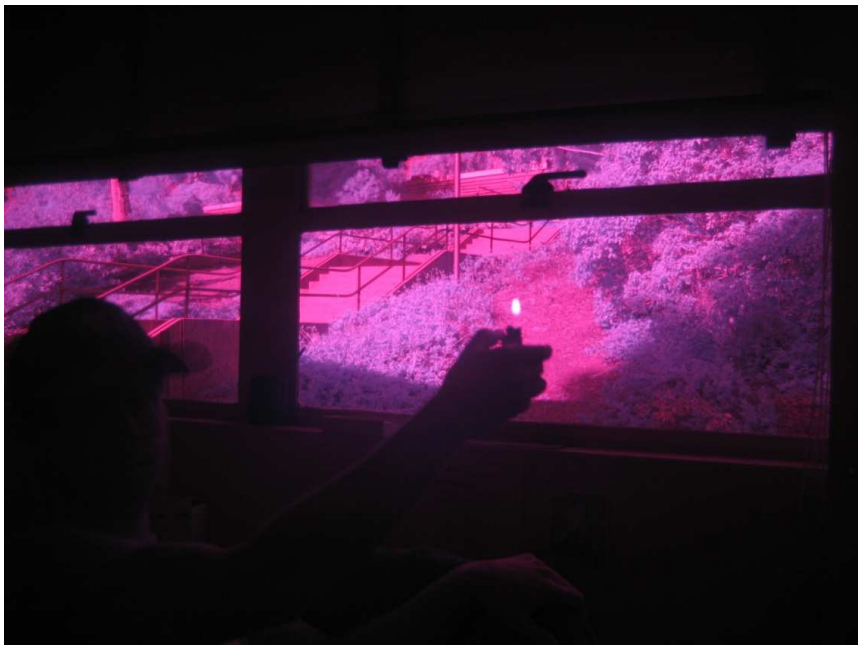

Figure 5: Powershot A95 with IR Filter

Figure 6: Photon 320 Lighter Test

The next tests occurred on March 4, 2010, and involved a small barbecue with wood as a fuel source. With this test we were able to test greater distances, up to 10 meters. Figure 7 shows two images taken with the Canon Powershot A95 camera. These images were taken at a range of approximately 10 meters. They show that although the IR pass filter dramatically increases the visibility of the flames, there is no additional visibility of the smoke or hot gasses generated by the fire. Figure 8 shows the same image taken with the FLIR camera. The heat of the fire is clearly visible against the cold background. Also, a small plume of hot gas is visible above the flame. This further confirms that the IR camera is able to see hot gas plumes if they exist. However, the plume is not as large as we originally had hoped. One potential reason for this is that the amount of fuel that we are burning in this test does not generate enough hot gas to create a large plume. Another possible reason is that atmospheric effects such as wind are dispersing the heat so quickly that there isn't enough concentrated heat energy to register on the camera.

On April 27, 2010 we repeated the barbecue test using cell phone cameras. The purpose of this test was to determine if cell phone cameras used different filters than the Powershot A95. The results of this test showed the same results as the March 4th test. The visible spectrum cameras were not sensitive enough to IR radiation to show a plume, and the lower resolution cameras on the cell phones used provided images of poor quality at any appreciable range.`

Figure 7: 10 Meter Test, With and without IR filter

Figure 8: 200 x 250 Close-up of Photon 320 at 10m showing Flame

Goleta Test

On May 8th, 2010 we went to the Goleta facility to perform an experiment with Raytheon. Used in the test was a Raytheon camera system as well as the camera systems we performed the previous tests with. The Raytheon system, the PS360, includes a visible spectrum, a SWIR camera, and a LWIR camera. The specifications of these cameras are listed in Figure 9. The test range was 832 meters long, with the camera systems mounted on a 60 foot tall tower looking down onto the target area. The target consisted of a 5 foot by 4 foot barbecue trailer that had a fire built inside of it. We also used a Ryobi IR001 Non-contact infrared thermometer to measure the temperature of the hot gas above the trailer.

Band	LWIR	SWIR	Visible
Sensor Resolution	640 x 480	640 x 512	4000 x 2650
Pixel Size	25 µm	25 µm	8 µm
Focal Length	77 mm	200 mm	200 mm
Size of pixel at target	27 cm	10 cm	3 cm

Figure 9: Specifications for PS360 cameras

We started the test by building a small charcoal fire at 9:23 AM, using approximately 10 pounds of charcoal in a 1.5 foot by 1 foot pile. Images were taken with all sensors. After the data was collected, the size of the fire was increased to a full 20 pounds of charcoal in a 2 foot by 2 foot pile. After waiting for the temperature to stabilize, we started collecting data at approximately 9:58 AM. During data collection the nature of the fire was changed by adding pine branches to the fire in order to create smoke. The fire size was increased a second time, to a total of 40 pounds of charcoal, in a 2 foot by 3 foot pile. The temperature stabilized at 10:20 AM, and similar data was collected. This time short sections of pine 2x4 pine boards were added to create smoke for a longer period. The size of the fire was then increased to 80 pounds and more pine wood added in a 3 foot by 3 foot pile. Data collection for this test was started at 10:43 AM. During this time, we were able to read the temperature of the air

above the fire at 161°F. Finally the fire was increased in size to 160 pounds of charcoal, covering the whole trailer. Data was taken at 11:13 AM. The temperature of the gas was varying between 115°F and 170°F at this point. The temperature of the gas continued to rise, reaching a maximum read temperature of 340°F before the termination of the experiment at 12:06 PM. At this point, the fire was extinguished using a large quantity of water, and the resulting steam cloud was captured by the Raytheon sensors. After it was confirmed the fire was completely out, the area was cleaned and the experiment was completed.

One potential issue that we discovered late in the test was that the grating above the trailer appeared to be acting as a heat sink, decreasing the heat of the gas plume rising from the fire. This could affect the visibility of the plume in the LWIR band by reducing the heat of the plume. There is no satisfactory method of determining if this reduced the usability of the data we collected. The only option we have is to analyze the data we have, and compare it to data collected in future tests where we don't have a grating present. Another problem that we had during the testing was our attempt to block the Raytheon camera from having a direct view of the fire using a set of tarps. The tarps were hoisted to form a vertical plane using two poles. The problem we had is that the tarps were reflective in the infrared range, causing the fire to become even larger on the LWIR sensor due to reflected radiation. This defeated the purpose of the tarps, which was to make the fire itself less visible, and hopefully accentuate the plumes. Once we realized this problem we removed the tarps and all of the data we collected was unaffected.

The results of this test initially indicated that a single spectrum of camera is not able to completely detect enough information to reliable detect a fire. The LWIR camera was unable to see any plume large enough to be readily visible to human inspection in real time. In contrast, the visible spectrum camera was able to easily see a plume of smoke, but the fire itself did not show any

particularly distinguishing characteristics. But examining the video files frame by frame, we were able to distinguish small plumes at a few different points. Figure 10 shows one of these small plumes with the plume highlighted for clarity. The plume is very faint, and difficult to see, which is why we missed it in the initial review of the data. However there was enough contrast to see it without any enhancement. The large plume that we saw was when we extinguished the fire. Figure 11 shows this plume. It is roughly the same size as the plume highlighted in Figure 10, but it has a much higher intensity on the camera, and therefore a higher temperature. The fact that we are able to see the steam plume so well is very important. It shows that it is possible to see a column of hot particulate matter, in this case water vapor particles, as they rise into the air off of a fire. With a sufficient quantity of smoke, and enough heat at the fire itself, we will be able to see a smoke plume rising from the fire.

Images were also taken at the Goleta test using the Photon 320 FLIR camera. Figure 12 shows excerpts from two images taken at different times from the same location approximately 50 meters away from the trailer. The image on the right shows a markedly larger flame than the image on the left, but more importantly, it also displays a very subtle plume of hot gas. The plume extends vertically and to the right. Figure 13 and Figure 14 show this plume more visibly. Figure 13 is the raw difference information comparing the two images from Figure 12. The images were imported into MATLAB, and a simple subtraction operation was performed. The plume and the fire are distinguishable features as well as a vertical shape to the right of the fire. That shape is a person who was in the field of view in one of the images, and missing in the other one. Figure 14 is the same difference image but converted to a binary format via thresholding. The threshold level was chosen to reduce the number of features in the image. It has not been optimized to create a binary image with the minimum number of features. This picture very clearly shows the plume as the primary feature in the image. Using a better decision algorithm an adaptive threshold could be chosen and this binary image could be used to detect a plume using an automated system.

The fact that this plume is readily visible using a few basic processing techniques gives great promise of the ability to detect fires using the multispectral system.

Figure 10: 832 meter small plume

Figure 11: Steam Plume at 832 meters

Figure 12: 190 x 175 Pixel Close-up of Photon 320 at 50m showing plume

Figure 13: Raw Difference image showing plume

Figure 14: Binary difference image showing plume

Conclusion

Fire detection is not an easy task to accomplish. We were able to gather important information on the spectral emissions of fire that will let us pick sensor technologies that will enable us to create a system that can reliably reduce the early detection rate of wildfires. Based on the preliminary results of our testing, a system using only one type of sensor does not appear to be adequate to detect a fire. A closer inspection revealed that there is enough data contained within the thermal IR band to detect a known fire, in controlled conditions. Because of the wide variety of lighting, weather, and terrain conditions in the real world, a single sensor system is still unlikely to be able to reliable detect a fire before it spreads beyond the point of easy containment. Therefore a multispectral system would be better. A combination of a standard visual range sensor and a thermal spectrum sensor is the optimal system based on the data we have acquired. The SWIR band did not appear to contain any useful information, but it has not been completely analyzed for spectral correlation or subtle features.

Future Work

With sensor types selected, and some valuable initial data collected, future work can now focus on continuing to collect data and developing algorithms to detect fires in the images. The method for fire detection that seems the most useful at this time is change detection on the thermal images. While observing the FLIR camera during the Goleta test, we noticed that the fire had a noticeable visible flicker. This flicker indicates that the fire changes both in size and intensity over time. By comparing the current image from the camera with the previous image that change can be detected. It is possible that a suitable threshold can be found that will distinguish a fire from other varying phenomenon. To determine that threshold, the frequency of the flicker must be calculated. By taking the Fourier transform of the temporal set of intensity values at the areas of interest, the frequencies can be found.

If the fire has a fairly constant frequency appearing in the flame over time, then that frequency can be filtered, and any set of images where this frequency occurs can be said to probably have a fire in the field of view. Another technique that can be used to help bring out the frequencies in the fire is time average filtering. The filtering effect could eliminate noise and subtle variations in the frequency, which could make determining threshold levels easier than with plain differencing data.

Another technique that can be applied is principle component analysis. Because we are using multiple cameras in multiple spectrums, we are able to use techniques that exploit the relationships between the different bands to extract information that isn't visible in any individual band. One prerequisite to this technique is spatially connecting the different bands. The same pixel in each picture must correspond to the same image feature in each band. In order to do this, the different spatial resolutions of the different cameras must be considered. The camera with the lowest resolution is the LWIR band, with a resolution of 26cm. The other two bands must be manipulated in some manner to match this. Either straight decimation can be used, dropping the extra pixels, but that leads to a high loss of useable data. A better method would be an averaging filter to average together pixels in the SWIR and visible bands to downscale their resolutions to 26cm. Using these multispectral techniques will allow us to examine the data from one set of bands in relationship to the data available in the other bands. A primary example of how this could be extremely beneficial is looking at the SWIR data from the Goleta test. While performing the test, we could detect almost no useful data in the SWIR band. Short wave infrared light passes through smoke and fog without any real distortion, which makes that type of phenomenon invisible in that band. Our observations on the live feed from the SWIR camera backed this up. However, there may be data in the image we cannot see with our eyes alone. By using the other bands, and spectrally decorrelating them, we may find that the SWIR band contains enough information about the fire to make detecting it easier than if we just had the thermal camera and the visible camera

Bibliography

Canon USA. (n.d.). *Digital Cameras - High-End, Advanced Digital Cameras - D-Series Digital Cameras - Performance and Style, Digital ELPH Cameras - Easy and Fun! A-Series Digital Cameras - Digital Camera - PowerShot A95 - Canon USA Consumer Products*. Retrieved May 1, 2010, from Canon USA Web site: http://www.usa.canon.com/consumer/controller?act=ModelInfoAct&fcategoryid=145&modelid=10468#ModelTechSpecsAct

FLIR. (n.d.). *Photon 320 Infrared Camera*. Retrieved April 28, 2010, from FLIR web site: http://www.flir.com/cvs/cores/uncooled/products/photon320/

Lillesand, T. M., Kiefer, R. W., & Chipman, J. W. (2008). *Remote Sensing and Image Interpretation* (Sixth ed.). John Wiley & Sons, Inc.

NASA. (n.d.). *Remote Sensing Tutorial*. Retrieved May 18, 2010, from NASA Web site: http://rst.gsfc.nasa.gov/Sect9/Sect9_2.html

NOAA. (n.d.). *NOAA Economics of Wild & Forest Fire Data and Products | Weather & Water | Extreme Events*. Retrieved April 28, 2010, from NOAA Econimics: http://www.economics.noaa.gov/?goal=weather&file=events/fire

Sun, H., Rong, Z., Lui, C., Liu, J., Zhang, Y., Zhang, P., et al. (2006). Spectral Characteristics of Infrared Radiation from Forest Fires. *Proceedings of SPIE - The International Society for Optical Engineering* .

Young, R. W. (2006, November 20). *Audit Report: Forest Service Large Fire Suppression Costs.* Retrieved May 1, 2010, from USDA web site: http://www.usda.gov/oig/webdocs/08601-44-SF.pdf

Appendix A: Matlab Code for Creating Binary Difference Image.

```
image1 = imread('10.12.50m.tif');
image2 = imread('10.13.50m.tif');
difference = image2-image1;
BW = im2bw(difference, 0.05);
Imwrite(difference,'diff.jpg','jpg');
imwrite(BW,'diffbw.jpg','jpg');
```